Multi-Objective Optimal D-PMU Placement for Fast, Reliable and High-Precision Observations of Active Distribution Networks

Yuce Sun [1], Wei Hu [2], Xiangyu Kong [1],* [ID], Yu Shen [2] and Fan Yang [2]

[1] Key Laboratory of Intelligent Power Grid Ministry of Education, Tianjin University, Tianjin 300072, China; eemliu@tju.edu.cn

[2] Electric Power Research Institute State Grid Hubei Electric Power, Wuhan 430077, China; huwei11@hb.sgcc.com.cn (W.H.); sheny20@hb.sgcc.com.cn (Y.S.); yangf81@hb.sgcc.com.cn (F.Y.)

* Correspondence: eekongxy@tju.edu.cn

Abstract: The distribution-level phasor measurement unit(D-PMU), as a new type of measurement equipment, can support the fast and high-precision observations of active distribution networks. This paper presents a new D-PMU optimal placement method that can be used to reconcile investments with the reliability of high-precision observation systems. The multi-objective optimization model primarily considers the influence of topology changes and N-1 contingencies on observation reliability. Its objectives include minimizing the number of D-PMUs, maximizing network measurement redundancy (NMR) and the average number of observable buses under N-1 contingencies (ANOBC). The model is extended to a form of multi-topology weighting and is combined with zero-injection buses and other measurements. We take the observability of high-weight topology set as the constraint. The model can be solved using the non-dominated sorting genetic algorithm-III (NSGA-III), which gives the set of Pareto optimal solutions. Then, the D-PMU placement order determination method based on the spatial electrical distance is proposed to improve the effect of state estimation faster. IEEE standard systems are taken to verify the effectiveness of the proposed method. With the same number of D-PMUs, this method derives more ANOBC and NMR than other methods. When considering topology changes, the proposed method can use fewer additional D-PMUs to substantially increase the ANOBC and NMR.

Keywords: D-PMU; active distribution network; observability; N-1 contingencies; non-dominated sorting genetic algorithm-III; topology change

1. Introduction

Traditional distribution network planning and operation methods cannot manage the large-scale access of distributed generations (DGs) and flexible loads. Distribution networks are evolving to become more flexible, reliable, efficient and intelligent [1]. However, current distribution networks lack sufficient measurement devices and rely heavily on pseudo measurements, which leads to poor state estimation accuracy and frequency. This low-frequency state estimation cannot meet the requirements of real-time control in intelligent distribution networks. As a monitoring device, a phasor measurement unit (PMU) can measure the voltage phasor and current phasor synchronously [2]. With the ability to provide phase angle data, along with a high sampling frequency and high data accuracy, the PMU is being widely applied in state estimation [2], faulted line identification [3], voltage monitoring [4] and other fields in smart grid.

If each bus of a power system installs a PMU, this system can be fully observable and can have a good state estimation capacity. However, PMUs are very expensive, which makes it difficult to install a large number of PMUs in a distribution network [5]. Exciting prospects are offered by the fact that the application of the distribution-level

phasor measurement unit (D-PMU) in distribution networks significantly reduces the costs of PMU placement [6]. This makes it possible to establish a wide-area measurement system in the distribution network. Nevertheless, due to a large number of distribution network nodes and changeable topology, the placement of D-PMU to ensure the observability of the network is still a huge investment. Therefore, the optimization of the placement of D-PMUs to support various functions of intelligent distribution networks, with limited investment, has become a research hotspot.

The current optimal D-PMU placement (OPP) methods for a distribution network focus on improving the observability of the power system and economic efficiency. Ref. [5] proposes an OPP method in the distribution network based on a meta heuristic algorithm and the effect of state estimation is verified. In Ref. [6], an OPP model for maximizing network observability is proposed, and the influence of distributed generation is considered. As the cost is related to the number of branches of the installed bus, an OPP method considering D-PMU installation costs and communication infrastructure is given in Ref. [7]. The solution is installed at multiple stages. Each stage depends on the cost of the utility setup rather than on the number of D-PMUs. In Ref. [8], considering all possible line connections of buses, a new D-PMU placement method for network observability is proposed. Ref. [9] uses the weak-load bus closeness criteria to determine the primary position at the beginning of D-PMU installation.

The above methods all operate on the premise that one D-PMU can indirectly observe multiple buses, but this mode of indirect observation reduces the reliability of the observation system. In addition, only satisfying observables may not meet state estimation needs. Therefore, some studies have considered network measurement redundancy (NMR) and have made full use of the existing advanced measurement infrastructure (AMI) and supervisory control and data acquisition (SCADA) measurements, which can improve observation reliability and reduce costs. Ref. [10] proposes a network compression method that combines existing measurements and reduces D-PMU candidate positions. Ref. [11] proposes an OPP model based on conventional measurements and D-PMU channel limitations to optimize the number and NMR. In Ref. [12], an OPP method based on a robust estimator is proposed, which can further increase the accuracy of system state estimation. In Ref. [13], considering existing measurements, a new OPP method is developed to enhance system observability. Two main methods are usually used to solve the OPP model: a numerical algorithm [14,15] and a heuristic algorithm [16,17]. The numerical algorithm has a fast calculation speed, but its universality is poor. Therefore, the numerical algorithm is mainly suitable for solving linear models. The heuristic algorithm has a strong global search ability and is mainly suitable for solving nonlinear, high-dimensional and multi-objective models.

However, although NMR can improve observation reliability to a certain extent, it cannot fully reflect the impact of various faults on system observations. The influences of line fault, D-PMU fault and other factors require more D-PMUs to ensure distribution network observability under different operating conditions. The *N*-1 contingencies resulting from D-PMU and line fault should be considered in the OPP problem. Ref. [18] considers the impact of power network expansion planning and line *N*-1 contingencies. Ref. [19] considers the impact of line *N*-2 contingencies. Ref. [20] takes observability under D-PMU *N*-1 contingencies as the constraint condition. Most of these references take observability under *N*-1 contingencies as a constraint and establish a single target and multi-constraint model.

However, there are three problems in the implementation of the above method:

(1) Realizing full observability under all contingency conditions is difficult. Many studies take system observability under *N*-1 contingencies as the constraint condition, which greatly increases the number of D-PMUs. When considering topology variation, the D-PMU number increase is more serious. It is necessary to find a compromise method in dealing with *N*-1 contingencies.

(2) Distribution network topology frequently changes, which may render the existing configuration unable to ensure observability after topology changes. Most of the

above OPP methods do not consider the current economic reconfiguration and future topology changes.

(3) D-PMU placement often faces the problem of insufficient funds in the short term. It is necessary to study how to better determine the placement order of D-PMUs in the placement scheme when short-term funds are insufficient.

To solve the above problems, a new OPP method for the distribution network is proposed in this paper. This method can not only improve the effect of D-PMUs on state estimation accuracy and frequency, but it can also improve the reliability of the distribution network measurement system. Firstly, we place D-PMU in advance on some important buses. Then, an OPP model is built based on the full usage of the existing measurement system, and, considering the topology changes, an OPP model is established to ensure complete observability of the main topologies, with the goal of improving economic efficiency, NMR and the average number of observable buses under contingencies (ANOBC). A solution based on non-dominated sorting genetic algorithm-III (NSGA-III) is proposed. A compromise solution that takes the above three objectives into account can be obtained in the Pareto solution set. Finally, in order to improve state estimation effectiveness faster, placement order is calculated based on the spatial electric distance. The proposed method successfully guides the D-PMU placement of the Nansha demonstration project in China. Compared with the existing methods, the main contributions of this method are as follows:

(1) An overall placement process of distribution network D-PMU is presented, which includes initial placement, overall placement and multistage placement.

(2) A topology generation method is proposed, which takes both the current and future economic reconfigurations of distribution networks into account.

(3) A multi-objective optimal D-PMU placement model considering topology changes and contingencies is proposed. The proposed model takes both zero-injection buses and other measurements into account, which not only minimizes the number of D-PMUs, but it also maximizes the ANOBC and NMR under the topology observability constraint. Compared with other methods, the proposed method can greatly reduce the D-PMU number with a high ANOBC and NMR.

(4) The NSGA-III algorithm gives the Pareto optimization solution set of the model. In addition, The Technique for Order Preference by Similarity to an Ideal Solution (TOPSIS) method is applied to select the optimal compromise solution.

(5) The placement order calculation method based on spatial electric distance is proposed, which can provide the D-PMU placement in order to improve the state estimation effect faster.

This paper is organized as follows: Section 2 presents the general framework of D-PMU placement and observability rules. Section 3 builds the multi-objective OPP model and the solution method based on NSGA-III. Section 4 proposes a placement order calculation method. In Section 5, simulations are carried out in IEEE standard systems to verify the efficiency of the proposed method. Section 6 gives the conclusion.

2. The Overall Strategy of D-PMU Placement

This section proposes the main process of D-PMU placement, the initial placement method and the observability rules.

2.1. The Overall Strategy of D-PMU Placement in Distribution Network

In order to realize the large-scale application and placement of D-PMU in the distribution network, the OPP method should not only take the effect of state estimation and economic efficiency into account, but it should also integrate with present measurement systems, such as SCADA and AMI. The existing measurement system is shown in Figure 1. D-PMU is generally installed on the bus of a medium-voltage distribution network. Different from SCADA and AMI, it can provide phasor information of bus voltage and branch current at high frequency. Therefore, the optimal placement of D-PMUs can realize dynamic observation of distribution networks. The key problem of OPP is studying which

buses should be placed with a D-PMU to realize reliable and dynamic observations of the distribution network.
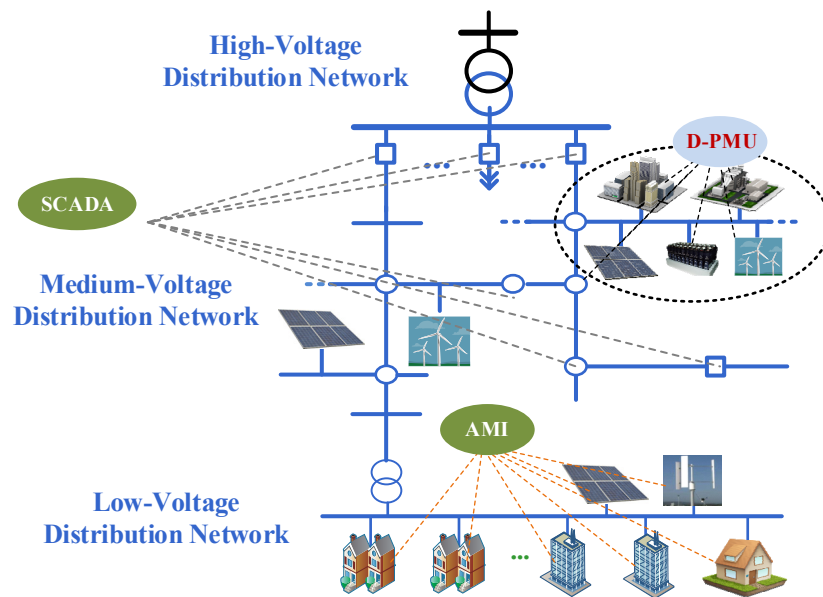
Figure 1. The structure of the existing measurement system.

In the optimization process, injection and power flow measurements provided by the SCADA system should be further applied to the OPP model, which can improve network observability [21]. AMI provides measurement data in the distribution network, such as node injection power pseudo-measurements. However, the sampling frequency of AMI measurements is low, and these measurements are usually used in the observability analysis of some non-essential areas of the distribution network.

With the continuous development of DGs and demand side management, the distribution network adjusts its network structure by operating segment switches and tie switches. This can reduce the cost of the system's operation and improve the consumption capacity of renewable energy. Therefore, the frequency of topological changes continues to increase. It is necessary to consider the impact of multiple topology observability on D-PMU placement.

Considering the factors above, the main process of D-PMU placement is shown in Figure 2. Firstly, some D-PMUs are preferentially placed on important buses. Secondly, an OPP model that can adapt to topology changes, and which is compatible with other measurement systems and can achieve multiple objectives, is established. Then, a corresponding intelligent algorithm is selected to solve the model. Finally, the most appropriate D-PMU placement order is calculated to guide the phased construction.
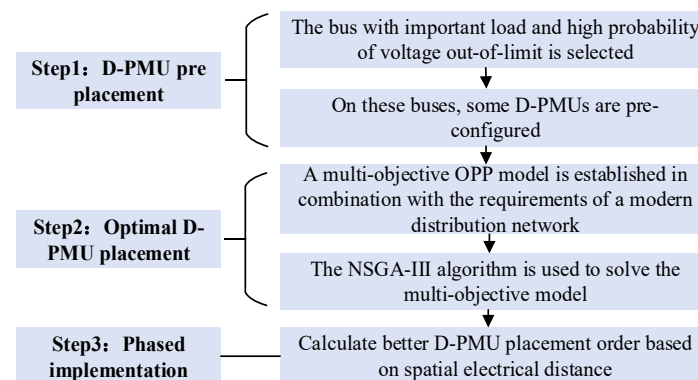
Figure 2. The main process of D-PMU placement.

2.2. Initial Placement of D-PMU

If a bus is identified that can cause personal casualties and heavy economic losses after power supply interruption, a D-PMU needs to be placed on the bus to monitor the operation status in real time. In addition, D-PMUs should be placed in advance according to practical applications, such as feeders with voltage regulating equipment, access points of photovoltaic power plants, etc. As a result of the access of new energy and electric vehicles, voltage instability caused by excessive voltage amplitude has become one of the main factors threatening the stable operation of the power grid. The real-time and accurate measurements of D-PMUs can capture the out-of-limit information of voltage in time. D-PMUs can be pre-placed on buses with a high probability of displaying out-of-limit voltage [15].

2.3. Analysis of the Observability

A D-PMU on a bus can provide the voltage phasor of the bus and the current phasors of associated branches. When the voltage phasor of a bus can be measured or calculated, the bus is observable. If all buses are observable, the network is fully observable. Supposing a D-PMU has enough channels, based on the Kirchhoff law and D-PMU characteristics, the observability rules are as follows:

(1) If a D-PMU is placed on a bus, this bus and its neighbors are observable, because for a bus with a D-PMU, the voltage phasor and current phasor of the associated branches are known, and the voltage phasors of its neighbors can be calculated by the Kirchhoff laws;

(2) If a ZIB is observable, and if only one neighbor's observability is unknown, the voltage phasor of this unknown neighbor can be calculated by the Kirchhoff laws. In other words, this neighbor is identified as observable;

(3) If all neighbors of a ZIB are observable, the voltage phasor of the ZIB can be calculated by the Kirchhoff laws.

3. Multi-Objective OPP Model

Considering the impact of *N*-1 contingencies and network reconfiguration, this paper builds a new multi-objective OPP model, which takes full observability as the constraint and takes the ANOBC, NMR and the number of D-PMUs as the objective functions. The model also considers the influence of ZIB and other measurements.

3.1. The First Objective Function Considering Economic Factors

In this model, the first goal of the OPP is to minimize the number of D-PMUs, which can be formulated as:

$$\min F_1(\boldsymbol{X}) = N_{\text{D-PMU}} = \sum_{i=1}^{N} x_i, \tag{1}$$

where N is the number of buses in the network, and i is the bus number. $N_{\text{D-PMU}}$ is the number of D-PMUs in the scheme. $\boldsymbol{X} = [x_1, x_2, \cdots x_N]^{\text{T}}$ is the N-dimensional column vector, whose entries x_i can be defined as:

$$x_i = \begin{cases} 0 & \text{bus } i \text{ has no D-PMU} \\ 1 & \text{bus } i \text{ has D-PMU} \end{cases} \tag{2}$$

3.2. The Second Objective Function Considering ANOBC
3.2.1. Line *N*-1 Contingencies and D-PMU *N*-1 Contingencies

N-1 contingencies include line *N*-1 contingencies and D-PMU *N*-1 contingencies. We can prove that, if the system is completely observable under D-PMU *N*-1 contingencies, the system is also completely observable under line *N*-1 contingencies. This principle is proven as follows.

When a single line of the distribution network fails, set P_1 is defined as the bus set connected to the bus i by only one line, and set P_2 is the bus set connected to bus i by two or more lines. The constraints that make the bus i observable are as follows (if bus i meets just one, it is considered observed):

(1) Bus i has a D-PMU;
(2) At least two buses in set P_1 have a D-PMU;
(3) At least one bus in set P_2 has a D-PMU.

The above constraints can be expressed as:

$$2x_i + \sum_{j \in P_1} x_j + 2\sum_{j \in P_2} x_j \geq 2 \quad i \in H_1, \tag{3}$$

where H_1 is the set of buses to be observed.

When any D-PMU of the distribution network fails, set P is defined as the bus set adjacent to bus i. At this time, the constraints that make bus i observable are as follows, and bus i can be observed when it meets one:

(1) Bus i has a D-PMU, and set P has at least one D-PMU;
(2) At least two buses in set P have a D-PMU.

The above constraints can be expressed as:

$$x_i + \sum_{j \in P} x_j \geq 2 \quad i \in H_1. \tag{4}$$

By comparing Equations (3) and (4), we see that, when each bus of the system can be observed under D-PMU N-1 contingencies, it must also be observable under line N-1 contingencies. This is because:

$$\sum_{j \in P} x_j = \sum_{j \in P_1} x_j + \sum_{j \in P_2} x_j, \tag{5}$$

$$2x_i + \sum_{j \in P_1} x_j + 2\sum_{j \in P_2} x_j - x_i - \sum_{j \in P} x_j = x_i + \sum_{j \in P_2} x_j \geq 0 \quad i \in H_1. \tag{6}$$

Therefore, when considering observability under N-1 contingencies, D-PMU N-1 contingencies are the main consideration.

3.2.2. Number of Observable Buses under D-PMU N-1 Contingencies

When one D-PMU fails, some buses in the network cannot be observed. The number of unobservable buses differs when the locations of D-PMUs are different. Ensuring the network is completely observable in the event of any D-PMU outages can double the number of D-PMUs that need to be provided. This is extremely uneconomical. Therefore, the second objective function is to maximize the average number of observable buses under D-PMU N-1 contingencies. This is taken as the value of the ANOBC.

Define X_S as the placement scheme, of which the total row number is $N_{\text{D-PMU}}$; Define X_{ok} as the k-th outage scheme, which is generated to simulate the N-1 contingencies. $N_{\text{D-PMU}}$ outage schemes are generated to simulate the N-1 contingencies. Using an IEEE 13-bus system as an example, if installing three D-PMUs in bus 2, bus 4 and bus 9, the placement scheme is $X_S = \begin{bmatrix} 0 & 1 & 0 & 1 & 0 & 0 & 0 & 0 & 1 & 0 & 0 & 0 & 0 \end{bmatrix}^T$, and the three outage schemes are defined as:

$$\begin{aligned} X_{o1} &= \begin{bmatrix} 0 & 0 & 0 & 1 & 0 & 0 & 0 & 0 & 1 & 0 & 0 & 0 & 0 \end{bmatrix}^T \\ X_{o2} &= \begin{bmatrix} 0 & 1 & 0 & 0 & 0 & 0 & 0 & 0 & 1 & 0 & 0 & 0 & 0 \end{bmatrix}^T . \\ X_{o3} &= \begin{bmatrix} 0 & 1 & 0 & 1 & 0 & 0 & 0 & 0 & 0 & 0 & 0 & 0 & 0 \end{bmatrix}^T \end{aligned} \tag{7}$$

The second objective function is calculated as:

$$\max F_2(\mathbf{X}) = ANOBCS = \sum_{k=1}^{N_{\text{D-PMU}}} n_{\text{o}k}/N_{\text{D-PMU}}, \tag{8}$$

where $n_{\text{o}k}$ is the number of observable buses of outage scheme $\mathbf{X}_{\text{o}k}$, which can be calculated as:

$$n_{\text{o}k} = \sum_{j=1}^{N} g_{\text{o}j}, \tag{9}$$

where $g_{\text{o}j}$ is a 0–1 auxiliary variable, which represents the observability of bus i, and is defined as:

$$g_{\text{o}j} = \begin{cases} 1 & m_{\text{o}j} \geq 1 \\ 0 & m_{\text{o}j} = 0 \end{cases}, \tag{10}$$

where $m_{\text{o}j}$ is the number of observations representing the NMR of bus j. The measurement redundancy vector $\mathbf{M}_{\text{o}k} = [m_{\text{o}1}, m_{\text{o}2}, \cdots m_{\text{o}N}]^{\text{T}}$ is calculated by:

$$\mathbf{M}_{\text{o}k} = \mathbf{A}\mathbf{X}_{\text{o}k}, \tag{11}$$

where $\mathbf{A}$ is the connectivity matrix, in which the elements are defined as follows:

$$\mathbf{A}(i,j) = \begin{cases} 1 & \text{ifbus } i \text{ is connected to bus } j \\ 1 & \text{if } i = j \\ 0 & \text{other} \end{cases}. \tag{12}$$

3.2.3. Impact of ZIB and SCADA

According to the observability rules proposed in Section 2.3, Equation (11) can be updated to:

$$\mathbf{M}_{\text{o}k} = \mathbf{A}\mathbf{X}_{\text{o}k} + \mathbf{O}_{\text{o}}, \tag{13}$$

where $\mathbf{O}_{\text{o}} = [o_{\text{o}i}]_{N \times 1}$ is the increased measurement redundancy of ZIB, which is a binary column vector. $o_{\text{o}i}$ can be calculated as follows according to the observability rules:

$$o_{\text{o}i} = \sum_{z=1}^{N_Z} u_{z,i}, \ u_{z,i} = \{0,1\}, \ z \in Z, \tag{14}$$

$$\sum_{i=1}^{N} u_{z,i} = \begin{cases} 1 \sum\limits_{i=1}^{N} A_{i,z} m_{\text{o}i} \geq \sum\limits_{i=1}^{N} A_{i,z} - 1 \\ 0 \sum\limits_{i=1}^{N} A_{i,z} m_{\text{o}i} < \sum\limits_{i=1}^{N} A_{i,z} - 1 \end{cases}, \ z \in Z, \tag{15}$$

where N_Z is the number of ZIBs; $u_{z,i}$ is a 0–1 auxiliary variable, indicating whether bus i can be observed by the ZIB characteristic of bus z; and Z is the ZIB number set.

When the power flow of branch p–q is measured by SCADA, we can calculate the voltage phasor at one end according to the voltage phasor at the other end. Thus, the measurement redundancy corresponding to the buses at the ends of branch p–q can be updated to:

$$\begin{aligned} m_{\text{o}p} &= \mathbf{A}_p \mathbf{X}_{\text{o}k} + o_{\text{o}p} + (1 - g_{\text{o}p}) g_{\text{o}q} \\ m_{\text{o}q} &= \mathbf{A}_q \mathbf{X}_{\text{o}k} + o_{\text{o}q} + (1 - g_{\text{o}q}) g_{\text{o}p} \end{aligned}, \tag{16}$$

where $\mathbf{A}_p$ and $\mathbf{A}_q$ are row p and row q of $\mathbf{A}$, respectively.

Buses whose injections can be measured by SCADA have the same characteristics, meaning that these buses can be treated as the ZIBs in the OPP model. As is expected, the realization of network observability combined with SCADA can induce a synchronization error. Therefore, the accuracy of state estimation should be verified after planning. If

the accuracy fails to meet the requirements, the considered number of SCADA should be appropriately reduced.

3.2.4. Observability of Non-Critical Bus Based on AMI Data

Making good use of the AMI system can also reduce the number of D-PMUs. AMI can realize the approximation of transformer load power according to user injection power. The specific steps are as follows:

For the feeder on the low-voltage side of the distribution transformer, the AMI system can record the power of each user every 15 min or 30 min. The sum power of all users on the feeder can be calculated as:

$$Q_c = \sum_i^Z Q_{Li} \quad P_c = \sum_i^Z P_{Li},\tag{17}$$

where Z is the number of users on the feeder; Q_c and P_c are the total reactive and active power of all users on the feeder, respectively; and Q_{Li} and P_{Li} represent the reactive and active powers of user i, respectively.

By calculating the sum of injection powers of all users of the lower-voltage distribution feeder, the pseudo-measurement data, i.e., the injection power of the combined distribution transformers, can be approximated. Therefore, the load power of buses can be calculated by using AMI measurements.

If the load power of a bus is known, and the connected buses of the bus are observable by placing D-PMUs, the voltage of the bus can be calculated by the Kirchhoff laws, which means that the bus can become observable by AMI data.

3.3. The Third Objective Function Considering NMR

Increasing the NMR can reduce the state estimation error. Therefore, maximizing the NMR is chosen as the third optimization objective, which is formulated as:

$$\max F_3(X) = NMR = \sum_{i=1}^N m_i, m_i = A(i,j)X(j) + o_i + \sum_{j=1}^{S_i} (1 - g_i)g_j.\tag{18}$$

where m_i is the number of observations of bus, and o_i is the increased measurement redundancy of ZIB, which is a binary vector. g_j represents the observability of bus i. The calculation method for these is similar to that which is applied in the case of D-PMU outage, such as Equations (8)–(14). S_i represents the number of SCADA branch measurements connected to the j-th bus.

3.4. The Constraints Considering the Network Observability

Realizing complete network observability is the constraint of the OPP model. The constraint can be calculated as:

$$M = AX + O + G \geq b,\tag{19}$$

where $M = [m_1, m_2, \cdots m_N]^{\mathrm{T}}$ is the measurement redundancy vector during the normal operation of each D-PMU and $O = [o_1, o_2, \cdots, o_N]^{\mathrm{T}}$; $b = [b_1, b_2, \cdots b_N]^{\mathrm{T}}$ is an N-dimensional column vector used to ensure that each bus is observable. G is the measurement redundancy added by SCADA, which is defined as:

$$G = \left[\sum_{i=1}^{S_1} (1 - g_1)g_i, \sum_{i=1}^{S_2} (1 - g_2)g_i, \cdots \sum_{i=1}^{S_n} (1 - g_n)g_i \right]^{\mathrm{T}},\tag{20}$$

In the existing OPP model, the buses in the network are not distinguished. Distribution networks may have multiple load buses. Considering the characteristics of different buses, the modified constraints are as follows:

$$b'_i = \begin{cases} 2 & \text{for D-PMU outage} \\ 1 & \text{for normal condition} \\ 0 & \text{for unimportant bus} \end{cases}. \tag{21}$$

Some important buses should be prioritized as the highest, such as hospitals, electrified railways and head offices. D-PMU outages can lead to the unavailability of measurements. In this study, the measurement redundancy of important buses is increased. These buses are observed at least twice, meaning that they can be observable under emergency conditions such as D-PMU outages. In contrast, some unimportant buses, such as affiliated workshops and public loads in small towns and rural areas, are not observed by D-PMUs in order to reduce the number of D-PMUs required. If some important buses need to be observable under emergency conditions, such as D-PMU outages, the values are taken as 2. If some unimportant buses do not need to be observable, the values of b'_i are taken as 0.

If the differences between buses are considered, b' can replace b to build a model. Although applying Equation (21) cannot provide a solution with the fewest D-PMUs, it can allow the D-PMUs to be placed more reasonably.

3.5. Multi-Objective OPP Model Considering Topology Changes

The frequent economic reconfiguration of a distribution network can change the network's topology, which means that D-PMUs may not be able to monitor adjacent nodes for a long time. Thus, the impact of economic reconfiguration on observability should be considered. The optimal reconfiguration of distribution systems with DGs helps attain multiple objectives, including load balancing, voltage profile improvements and loss reduction [22–25]. Equation (22) considers current profile improvements, voltage profile improvements and loss reduction [23–25]. The three parts of (22) are respectively derived from [22–25]. The objective function is formulated as follows:

$$F = u_{load} \cdot \sum_i^{N_{br}} \left(\frac{I_i - I_{ave}}{I_{ave}} \right)^2 + u_{voltage} \cdot \sum_i^N \left(\frac{V_i - V_{Ni}}{V_{Ni}} \right)^2 + u_{loss} \cdot \left(\sum_i^{N_{br}} \left| I_i^2 \right| \cdot r_i / P_{loss0} \right), \tag{22}$$

where N_{br} is the number of branches; I_i is the current of the i-th branch, I_{ave} is the average current of all branches; V_i and V_{Ni} are the true and reference voltage of the i-th bus; r_i is the resistance of the i-th branch; P_{loss0} is the power loss of the normal network's topology; and u_{load}, $u_{voltage}$ and u_{loss} are the weights of different optimal objectives.

If the load distribution and network parameters are known in each reconfiguration period, the optimal reconfiguration scheme can be calculated according to Equation (22). Ref. [26] provides a load forecasting method that can predict the probability of load distribution in multiple time scales. The scene set of distributed generation outputs and load distributions can be produced by the Monte Carlo simulation combined with distributed generation output forecasting, which is considered a reconfigured topology set in the proposed OPP model. Then, the topology weight can be calculated according to the frequency of each topology during the simulation. Each topology weight is: $\alpha_1, \alpha_2, \ldots, \alpha_R$.

Therefore, each objective function can be changed to the average value under the main topologies to ensure good performance of the placement scheme under multiple topologies. The OPP model can be updated to:

$$\min F_1(\boldsymbol{X}) = N_{\text{D-PMU}} = \sum_{i=1}^{N} x_i$$
$$\max F_2(\boldsymbol{X}) = NOBCS = \sum_{c=1}^{R} \sum_{k=1}^{N_{\text{PMU}}} \alpha_c n_{\text{oc},k} / (N_{\text{D-PMU}} \cdot R)$$
$$\max F_3(\boldsymbol{X}) = NMR = \sum_{c=1}^{R} \sum_{i=1}^{N} \alpha_c m_{ci} / R$$
$$s.t. \, \boldsymbol{M}_c \geq \boldsymbol{b} \, c = 1, 2, \cdots, R$$

(23)

where R is the number of topologies considered in the model; c is the topology number; $n_{\text{oc},k}$ is the value of $n_{\text{o},k}$ under the c-th topology; m_{ci} is the value of m_i under the c-th topology; and $\boldsymbol{M}_c$ is the measurement redundancy vector $\boldsymbol{M}$ under the c-th topology. The three objective functions in Equation (23) correspond to the weighted average of the three objective functions in Sections 3.1–3.3 under multi-topology.

If there are special requirements for the accuracy of state estimation, the influence of inherent accuracy and environmental noise on measurement placement should be considered. In Ref. [10], we proposed a state estimation error calculation method using mixed measurements. The state estimation error calculated by this method can be used as a constraint to meet the needs of state estimation. Limited by the length of the paper, we do not discuss this method in detail.

3.6. Solution Methodology Based on NSGA-III

The above model describes a nonlinear, multi-objective optimization problem. Multi-objective problems usually have a series of solutions, which are called non-dominated solution sets. A model with two objective functions can be solved by the non-dominated sorting genetic algorithm II (NSGA-II). However, if NSGA-II is used to solve the model with three or more objective functions, the non-uniform distribution of the Pareto solution at the non-dominated level makes it easy to fall into local optimization. Therefore, the NSGA-III is used to solve this problem.

NSGA-III and NSGA-II have a similar algorithmic framework. However, NSGA-III uses a method based on reference points to choose individuals, which is distinguished from NSGA-II.

The process of NSGA-III includes nondominated sorting, the determination of reference points, the adaptive normalization of individuals, association to reference points and niche-preservation operations. The calculation method can be found in Refs. [27–29]. The key step is the determination of reference points. The calculation method in this paper is as follows:

The number of reference points that are generated depends on the number of objective functions l and on another positive integer H, which can be defined as:

$$\sum_{i=1}^{l} y_i = H, y_i \in \{0, 1, 2, \ldots H\}, i = 1, 2, \cdots, l,$$

(24)

where the number of objective functions l is 3.

The number of solutions N_x of Equation (24) is calculated as:

$$N_x = \binom{H + l - 1}{l - 1}.$$

(25)

Assuming that $Y_j = \left(y_{j,1}, y_{j,2}, \cdots, y_{j,l} \right)^{\text{T}}$ is the j-th solution of Equation (24), the reference point $\lambda_{j,k}$ can be obtained as:

$$\lambda_{j,k} = \frac{y_{j,k}}{H}, \, k = 1, 2, \cdots, l.$$

(26)

NSGA-III can obtain the Pareto optimal solution set, which can make at least one target better without deteriorating any target. We cannot find a better solution outside the Pareto solution set. A scheme can be selected according to our requirements. For example, when two objectives have certain requirements, the third objective is the best and can be directly derived from the solution set.

Then, TOPSIS is applied to select the compromise solution. The standardized decision matrix can be obtained by referring to Ref. [30]. The ideal solution can be obtained by calculating the maximum value of each decision matrix column. The distances from each individual to the positive and negative ideal solutions are calculated according to Equation (27). The ideality is calculated according to Equation (28) for all Pareto optimal solutions. Finally, the Pareto solution with the largest ideality is selected as the compromise optimal solution.

$$d_i^+ = \|z_i - Y^+\| d_i^- = \|z_i - Y^-\| \ i = 1, 2, \cdots, Q, \tag{27}$$

$$D_i = \frac{d_i^-}{d_i^+ + d_i^-} \ i = 1, 2, \cdots, Q, \tag{28}$$

where d_i^+ and d_i^- are the distances from the i-th Pareto optimal solution to the positive and negative ideal solutions Y^+ and Y^-, respectively and z_i is the i-th Pareto optimal solution. D_i is the ideality of the i-th Pareto optimal solution.

4. D-PMU Placement Order Determination Based on Spatial Electrical Distance

To ensure that the network is completely observable, the number of buses installed with D-PMUs accounts for a higher proportion of the total number of buses, generally more than one-third. Therefore, it is difficult to implement the whole solution of OPP at the same time.

If a bus is installed with a D-PMU, the state estimation error variance of this bus is most significantly reduced due to the high accuracy of the D-PMU. Moreover, the state estimation accuracy of those buses which are close to the D-PMU bus is also significantly improved. The higher that the accuracy of the D-PMU's data are, the greater that the improvement in state estimation is. In contrast, the state estimation accuracy improvement of those buses which are not close to the D-PMU bus is not obvious. In order to ensure that the OPP method is easily applied in practical engineering, the D-PMU placement order determination method based on spatial electrical distance is proposed to maximize the state estimation accuracy of each stage. The reciprocal of the spatial electrical distance between the bus where the D-PMU is installed and the newly observable bus is selected as the weight. The greater that the weight of the location is, the higher that the priority of the installed D-PMU is.

4.1. Spatial Electrical Distance

Traditional electrical distance characterizes the closeness of electrical connections between two buses. Spatial electrical distance considers the influence of various buses in the system.

There are many ways to define electrical distances, most of which are defined as the sensitivity of reactive power variations to the voltage amplitude magnitude. However, this kind of method is defined as applied to voltage control. Voltage amplitude can be measured directly, and the phase angle needs to be measured indirectly in a traditional power grid. Therefore, state estimation can pay more attention to phase angle than to amplitude. In addition, compared with SCADA, the D-PMU can measure phase angle data. In state estimation with D-PMU data, the D-PMU can significantly improve the accuracy of the phase angle data.

Therefore, this paper uses the formula characterizing the effect of active power variations on the voltage phase angle to calculate the spatial electrical distance. This method

can improve the phase angle estimation accuracy as rapidly as possible during the D-PMU placement stages.

Based on the traditional power flow equation, keeping the reactive power constant, the sensitivity of the active power to the voltage phase angle can be expressed as:

$$\Delta \delta = \mathbf{S} \Delta \mathbf{P} = \left[\mathbf{H} - \mathbf{N} \mathbf{L}^{-1} \mathbf{J} \right]^{-1} \Delta \mathbf{P}, \tag{29}$$

where $\Delta \delta$ is the variation of the bus voltage phase angle and $\mathbf{S} = \left[\mathbf{H} - \mathbf{N} \mathbf{L}^{-1} \mathbf{J} \right]^{-1}$ is the sensitivity matrix, which represents the sensitivity of active power variation to voltage phase angle variation. $\Delta \mathbf{P}$ is the bus active power variation vector, and $\mathbf{H}$, $\mathbf{N}$, $\mathbf{J}$ and $\mathbf{L}$ are Jacobian submatrices, of which coefficients are real numbers.

According to the sensitivity matrix $\mathbf{S}$, the sensitivity between buses can be calculated as:

$$k_{ij} = \left| \lg \left(\frac{S_{jj}}{S_{ij}} \right) \right|, \tag{30}$$

where k_{ij} represents the voltage phase angle variation ratio between bus i and j when bus j active power changes. The larger that k_{ij} is, the smaller that the effect of bus j is on bus i voltage phase angle.

According to k_{ij}, the associated sensitivity matrix $\mathbf{K}$ is calculated as:

$$\mathbf{K} = \left[k_{ij} \right]_{n \times n} = \begin{bmatrix} k_{1,1} & k_{1,2} & \cdots & k_{1,n-1} & k_{1,n} \\ k_{2,1} & k_{2,2} & \cdots & k_{2,n-1} & k_{2,n} \\ \vdots & \vdots & \cdots & \vdots & \vdots \\ k_{n-1,1} & k_{n-1,2} & \cdots & k_{n-1,n-1} & k_{n-1,n} \\ k_{n,1} & k_{n,2} & \cdots & k_{n,n-1} & k_{n,n} \end{bmatrix}, \tag{31}$$

where n is the number of buses in the network.

According to the matrix $\mathbf{K}$, the Euclidean distance between buses i and j is calculated as:

$$\begin{aligned} d_{ij} &= \| \mathbf{k}_i - \mathbf{k}_j \|_2 \\ &= \left[(k_{i1} - k_{j1})^2 + (k_{i2} - k_{j2})^2 + \cdots + (k_{in} - k_{jn})^2 \right]^{1/2} \end{aligned} \tag{32}$$

where d_{ij} is the spatial electrical distance between buses i and j. The smaller that d_{ij} is, the greater that the influence of bus j is on bus i voltage phase angle, and the closer that the electrical connection is. In contrast, the higher that d_{ij} is, the greater that the electrical coupling degree is between buses i and j.

According to spatial electrical distance d_{ij}, the associated weight between buses i and j is defined as w_{ij}:

$$w_{ij} = d_{ij}^{-1}. \tag{33}$$

If topology variation is considered, the above formula is modified as:

$$w_{ij} = \sum_{c=1}^{R} a_c d_{cij}^{-1}. \tag{34}$$

where d_{cij} is the spatial electrical distance between bus i and j under the c-th topology.

4.2. Determining the Order of D-PMUs

According to the spatial electrical distance between the buses, the order of placement of D-PMUs can be determined to maximize the state estimation accuracy during each D-PMU placement stage. The specific steps of the determination method are as follows:

(1) All buses in the optimal solution that need to be installed with D-PMU are combined into a candidate set;

(2) For each bus in the candidate set, all newly added observable buses should be found after the given bus has been assigned a D-PMU;

(3) By summing the associated weights w_{ij} of the bus with those of the newly added observable buses, the integrated weight C_i is obtained;

(4) The bus with the largest value of C_i is chosen as the next location for installing the D-PMU. Then, this bus is removed from the candidate set;

(5) Is the candidate set empty? If the answer is yes, end. If the answer is no, go to step 2.

The flow of the proposed OPP method is shown in Figure 3.
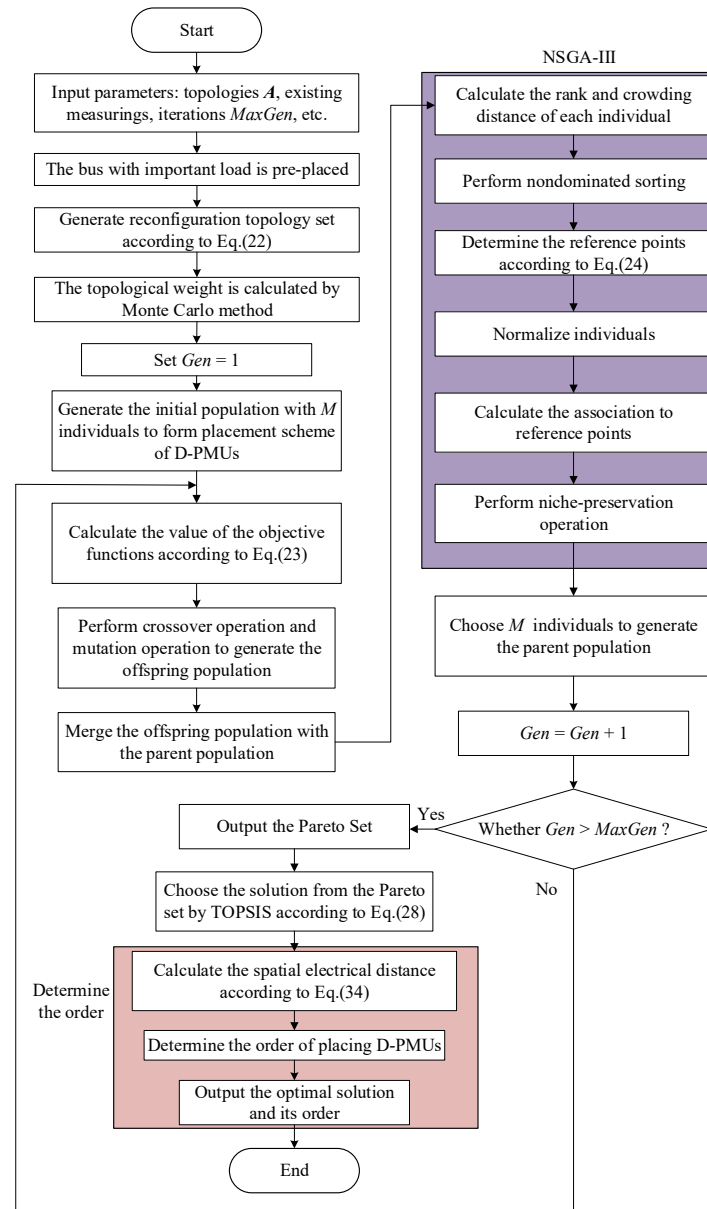
Figure 3. The proposed OPP method flow chart.

5. Simulation Results

5.1. The Pareto Solution Set Based on NSGA-III

The simulation results of two IEEE standard bus systems show the efficiency of the OPP method. Appendix A shows the topology of the IEEE 33-bus system. The bus number is 1–33, and s1–s37 is the switch number. Two topologies are considered temporarily; switches 7, 9 and 14 are opened; and switches 33, 34 and 35 are closed to form the second

topology. The existing ZIBs are injection measurements of buses 5, 6 and 21. Power flow measurements are branches 2–19 and 28–29. Bus 2 has been pre-placed with a D-PMU.

The NSGA-III algorithm is applied to solve the proposed model. In detail, the number of iterations is assigned to 1000. The number of individuals in the group is set to 100. The initial probabilities of the operation mutation and crossover operation are assigned to 0.4 and 0.8, respectively. In this paper, the NSGA-III algorithm is programmed with MATLAB software. The presented model is tested on a computer with an intel core i3 CPU and 2.0 GB of RAM.

The Pareto set obtained by the proposed method is shown in Figure 4. The optimal solution can be selected according to the needs. For example, for any given NMR and ANOBC, the solution with the smallest number of D-PMUs can be found from the solution set in Figure 4. In order to facilitate comparison, the $N_{D\text{-}PMU}$ is taken as the primary goal, and the remaining goals are selected by the TOPSIS method. The compromised optimal solution is the point marked by the red star in Figure 4.
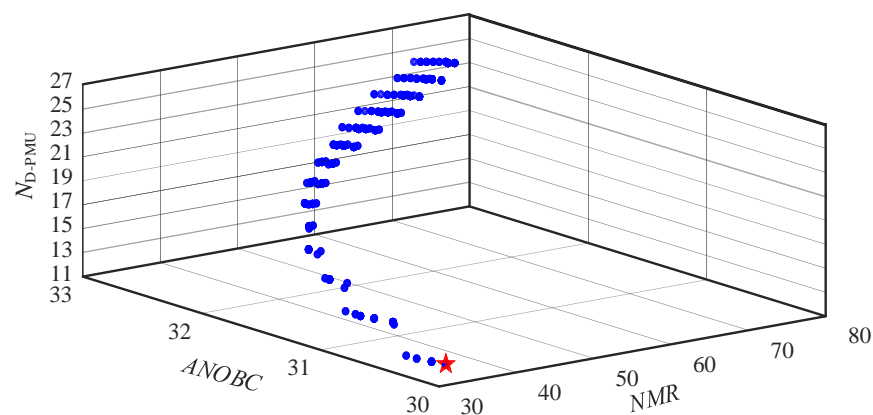
Figure 4. The Pareto set and the compromised optimal solution.

According to Figure 4, considering SCADA, ZIB and two topologies, the compromised optimal solution of OPP requires 11 D-PMUs. Through the D-PMU placement order determination method in Section 4, the order of placing D-PMUs is given, which can maximize the state estimation accuracy of each installation stage. The D-PMU placement order according to the sequential calculation method is: 3, 26, 14, 9, 17, 20, 29, 32, 11, 2, 24.

Figure 5 shows the application result of the proposed method for the IEEE 33-bus system. The D-PMU of bus 2 can observe bus 1, 2, 3 and 19; the D-PMU of bus 3 can observe bus 4 and 23; and the D-PMU of bus 26 can observe bus 6, 26 and 27; bus 9, 11, 14 and 17 can observe bus 8 to 18; the D-PMU of bus 20 can observe bus 20 and 21; the D-PMU of bus 24 can observe bus 23 and 25; and the D-PMU of bus 29 and 32 can observe bus 28 to 33. Because bus 4 and 6 are observed, and because bus 5 has injection power measurement equipment, bus 5 is observed. Similarly, 7 and 22 are observable based on the D-PMUs of bus 5, 6 and 26 and of bus 20 and 21, respectively. So far, the whole topology is considerable. Similar to the analysis of the second topology after switching, the observability of the whole topology can also be proved. Therefore, the whole network's observability under multiple topologies is realized.
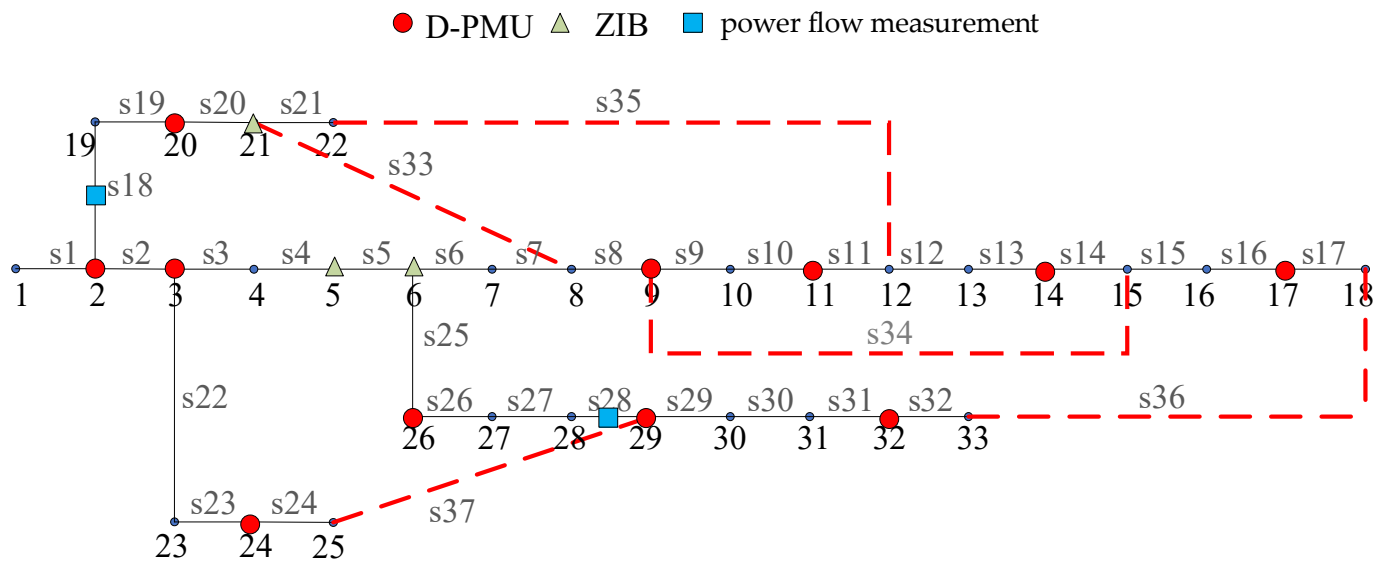
Figure 5. Results of D-PMU placement for IEEE 33-bus system.

5.2. Method Comparison

When choosing NSGA-II as the comparison algorithm, the proposed OPP methods based on NSGA-III and NSGA-II are individually simulated on the IEEE 33-bus system. Table 1 shows the comparison results between different methods. Compared with other algorithms, the proposed algorithm can achieve more ANOBC and NMR. Compared with the OPP method based on NSGA-II, the proposed OPP method based on NSGA-III can obtain a better solution with a higher NMR and a higher ANOBC. In addition, it can be seen from Table 1 that NSGA-III takes the shortest time because it has a faster convergence speed than NSGA-II. Therefore, compared with NSGA-II, NSGA-III is more suitable for optimizing the proposed multi-objective model of OPP.

Table 1. Comparison of results based on different methods.

Algorithm	Num. of D-PMUs	ANOBC	NMR	Execution Time/s
NSGA-III	11	30.64	36.5	2.3503
NSGA-II	11	30.36	35.5	2.6363
NSGA-II (Only consider num)	11	28.68	34.5	2.3728

According to the measurement data from before and after the installation of the D-PMU, we carry out 1000 state estimation simulations. Pseudo measurements, SCADA and D-PMU accuracy have been derived from Refs. [10,31]. The relative error is calculated according to the true value of power flow and the result of state estimation. The average estimation errors in the voltage amplitude and phase angle of each bus are effectively reduced by implementing the D-PMU placement scheme, which is shown in Figures 6 and 7. This is because the D-PMU has higher accuracy than traditional measurements and the ability to directly measure the phase angle. The state estimation results without D-PMUs are the state estimation results of replacing D-PMUs with SCADA measurements.

In order to better reflect the advantages of the proposed method, several indexes considered in this paper are compared with the method from Refs. [32,33] in IEEE 33- and 69-bus systems. Tables 2–4 show the comparison results. Appendix A Figure A2 shows the topology of the IEEE 69-bus system.
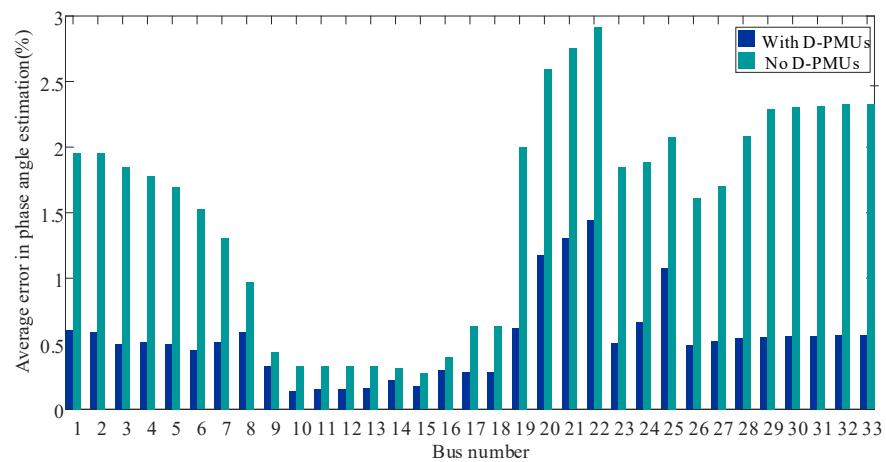
Figure 6. Comparison of average errors in voltage amplitude.
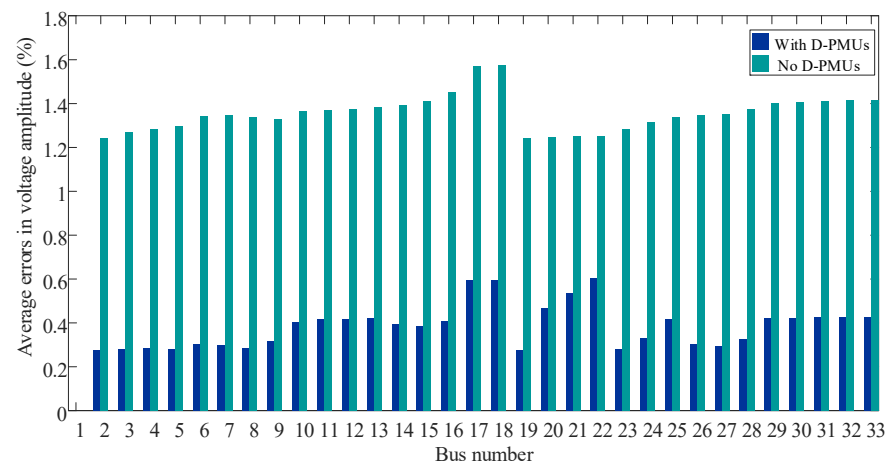
Figure 7. Comparison of average errors in voltage phase angle.

Table 2. Comparison of the minimum number of D-PMUs for complete observability.

Method	IEEE 33-Bus System		IEEE 69-Bus System	
	Num	D-PMU Locations	Num	D-PMU Locations
Proposed Method	11	2, 3, 9, 11, 14, 17, 20, 24, 26, 29, 32	24	2, 3, 8, 13, 16, 19, 23, 26, 30, 34, 37, 40, 43, 45, 49, 51, 53, 56, 59, 60, 63, 64, 66, 68
Ref. [32]	14	2, 4, 6, 8, 11, 13, 15, 17, 21, 23, 24, 27, 29, 32	27	1, 4, 5, 8, 9, 12, 15, 18, 20, 23, 26, 29, 32, 34, 37, 40, 42, 45, 49, 52, 53, 55, 58, 61, 64, 66, 69
Ref. [33]	11	2, 6, 8, 11, 15, 17, 21, 24, 28, 29, 32	26	1, 4, 8, 14, 17, 19, 21, 24, 27, 28, 31, 34, 37, 39, 42, 45, 49, 51, 54, 56, 59, 61, 64, 66, 68, 69

Table 3. Comparison of multiple indicators of IEEE 33-bus system.

Method	IEEE 33-Bus System			
	NMR	Observability of Topology		ANOBC
		Topology 1	Topology 2	
Proposed Method	36.5	Yes	Yes	30.64
Ref. [32]	45.0	Yes	Yes	31.64
Ref. [33]	37.5	Yes	No	29.54

Table 4. Comparison of multiple indicators of IEEE 69-bus system.

Method	IEEE 69-Bus System			
	NMR	Observability of Topology		ANOBC
		1	2	
Proposed Method	77.5	Yes	Yes	62.63
Ref. [32]	81.0	Yes	Yes	65.68
Ref. [33]	79.0	Yes	No	65.07

According to Table 2, the proposed method uses fewer D-PMUs than other methods. According to Tables 3 and 4, the proposed algorithm improves NMR and the ANOBC as much as possible while ensuring the complete observability of multiple topologies. NMR and the ANOBC are not integers because they are the average of multiple topologies. With the same number of installations, the proposed method derives more ANOBC.

5.3. The Influence of Topology Number

The topology generation method used in this paper has been applied to the IEEE 33-bus system. According to the operation data of the distribution network in Refs. [25,26], the generated reconfigured topologies are obtained by a Monte Carlo simulation that has been run 2000 times. We select the topologies with a proportion of occurrence over 0.08, and we finally derive 11 topologies, as shown in Table 5. Method 2 is used to realize network observability without considering accidental faults. Method 3 is used to realize complete observability under N-1 D-PMU outages. According to the proposed method, the optimal compromise solution with a maximum cost of 20% compared with method 2 is selected from the Pareto solution set. The variation relation between the three objective functions and the number of topologies is as shown in Figures 8–10.

Table 5. The topological set of IEEE 33-bus system used.

Topology	IEEE 33-Bus System	
	Closed	Open
1	no	no
2	s33, s34, s35	s7, s9, s14
3	s35, s37	s7, s25
4	s34, s36	s13, s17
5	s33, s37	s5, s26
6	s36, s37	s16, s25
7	s36, s37	s24, s31
8	s33, s34, s35	s6, s11, s12
9	s34, s36	s14, s15
10	s35, s37	s2, s3
11	s34, s36, s37	s12, s23, s27

According to Figure 8, after the number of topologies increases to eight, the number of D-PMUs that must be placed does not increase. The reason is that, when the number of D-PMUs is high, the system has high measurement redundancy, which increases the reliability of system observation. According to Figures 8–10, the proposed method can increase the ANOBC to near the average number of methods 2 and 3 at the cost of increasing the D-PMU number by 20%. The NMR is also increased by about 30% compared with Method 2. Although the more popular Method 3 can maximize the ANOBC, it increases the number about twofold compared with Method 2. When the number of topologies

reaches seven, Method 3 ensures that almost every bus is equipped with a D-PMU, which is extremely uneconomical. Therefore, it can be concluded that, compared with other methods, the proposed method can greatly improve the ANOBC and NMR with a small increase in the number of D-PMUs. There are two main reasons. On one hand, the greater that the number of D-PMU configurations is, the stronger that the ability of the system to maintain observability is in cases of topology change and component failure. On the other hand, reasonable D-PMU placement can reduce the demand for measurement quantity.
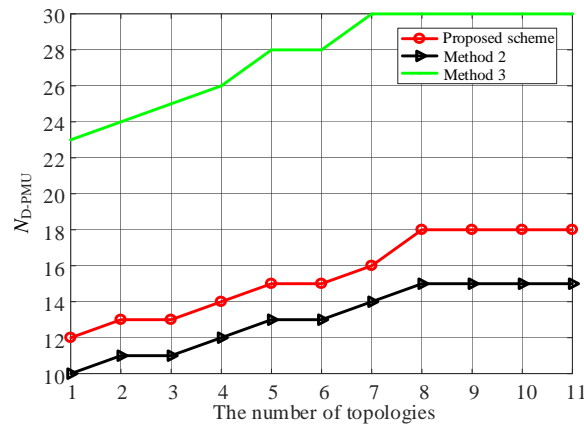
Figure 8. Relationship between $N_{\text{D-PMU}}$ and the number of topologies.
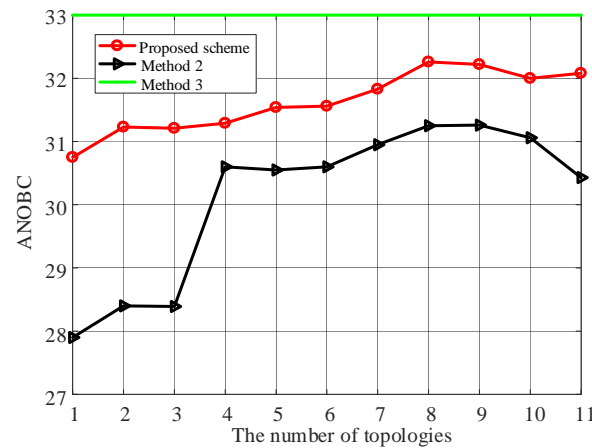
Figure 9. Relationship between ANOBC and the number of topologies.
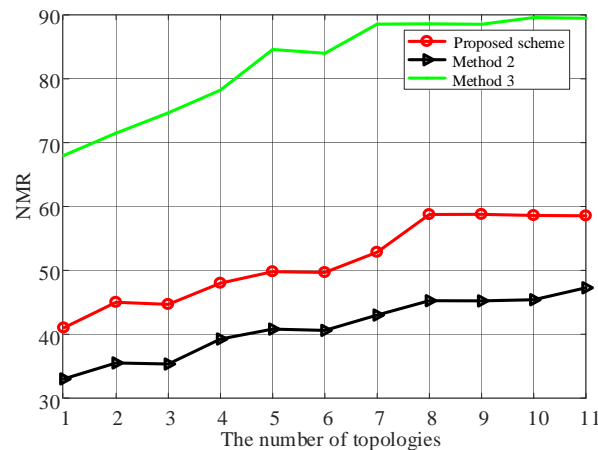
Figure 10. Relationship between NMR and the number of topologies.

6. Conclusions

This paper presents a novel D-PMU placement method that involves three processes: initial distribution, overall scheme and phased implementation. Considering current and future distribution network reconfiguration, a multi-objective optimal placement model of D-PMUs is built to minimize the number of D-PMUs and to maximize the NMR and the ANOBC. The Pareto optimization solution set of the model is given by NSGA-III, and the compromise optimal solution is selected by TOPSIS. The placement order is based on the spatial electrical distance. The effectiveness of the method is verified in IEEE 33- and 69-bus systems. The results show that the NSGA-III algorithm outperforms the traditional NSGA-II algorithm in terms of solution time and finding the global optimal solution. With the same number of D-PMUs, the proposed method derives more ANOBC and NMR than other methods. When considering topology changes, the proposed method can use fewer additional D-PMUs to substantially increase the ANOBC and NMR, because a better placement of D-PMUs can reduce the number of D-PMUs required.

Author Contributions: Methodology, writing—review, editing software, validation, Y.S. (Yuce Sun); writing—review and editing, Y.S. (Yu Shen), W.H., F.Y. and X.K.; conceptualization and writing—original draft preparation, Y.S. (Yuce Sun). All authors have read and agreed to the published version of the manuscript.

Institutional Review Board Statement: Not applicable.

Informed Consent Statement: Not applicable.

Data Availability Statement: Not applicable.

Conflicts of Interest: The authors declare no conflict of interest.

Appendix A
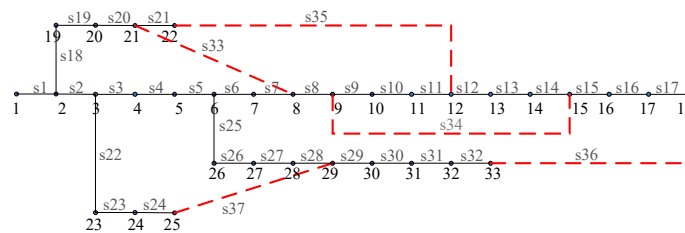
Figure A1. IEEE 33-bus system.
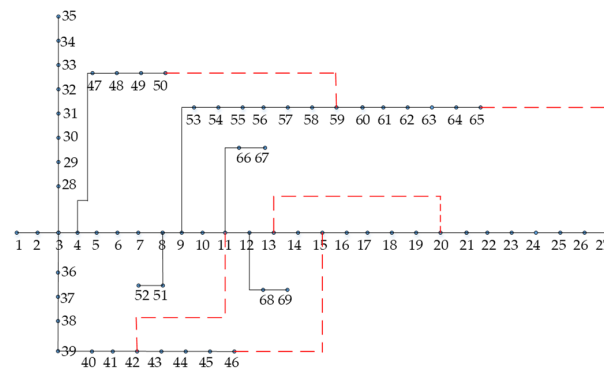
Figure A2. IEEE 69-bus system.

References

1. Kong, X.; Xu, Y.; Jiao, Z.; Dong, D.; Yuan, X.; Li, S. Fault Location Technology for Power System Based on Information about the Power Internet of Things. *IEEE Trans. Ind. Inform.* **2020**, *16*, 6682–6692. [CrossRef]
2. Ahmed, M.M.; Amjad, M.; Qureshi, M.A.; Imran, K.; Haider, Z.M.; Khan, M.O. A Critical Review of State-of-the-Art Optimal PMU Placement Techniques. *Energies* **2022**, *15*, 2125. [CrossRef]
3. Joshi, P.M.; Verma, H.K. Synchrophasor measurement applications and optimal D-PMU placement: A review. *Electr. Power Syst. Res.* **2021**, *199*, 107428. [CrossRef]
4. Lambrou, C.; Mandoulidis, P.; Vournas, C. Validation of Voltage Instability Detection and Control Using a Real Power System Incident. *Energies* **2021**, *14*, 7165. [CrossRef]
5. Lee, K.-Y.; Park, J.-S.; Kim, Y.-S. Optimal Placement of D-PMU to Enhance Supervised Learning-Based Pseudo-Measurement Modelling Accuracy in Distribution Network. *Energies* **2021**, *14*, 7767. [CrossRef]
6. Chauhan, K.; Sodhi, R. Placement of Distribution-Level Phasor Measurements for Topological Observability and Monitoring of Active Distribution Networks. *IEEE Trans. Instrum. Meas.* **2019**, *69*, 3451–3460. [CrossRef]
7. Almasabi, S.; Mitra, J. Multistage Optimal D-PMU Placement Considering Substation Infrastructure. *IEEE Trans. Ind. Appl.* **2018**, *54*, 6519–6528. [CrossRef]
8. Khorram, E.; Jelodar, M.T. D-PMU placement considering various arrangements of lines connections at complex buses. *Int. J. Electr. Power Energy Syst.* **2018**, *94*, 97–103. [CrossRef]
9. Kumar, S.; Tyagi, B.; Kumar, V.; Chohan, S. Optimization of Phasor Measurement Units Placement Under Contingency Using Reliability of Network Components. *IEEE Trans. Instrum. Meas.* **2020**, *69*, 9893–9906. [CrossRef]
10. Kong, X.; Wang, Y.; Yuan, X.; Yu, L. Multi Objective for D-PMU Placement in Compressed Distribution Network Considering Cost and Accuracy of State Estimation. *Appl. Sci.* **2019**, *9*, 1515. [CrossRef]
11. Manousakis, N.M.; Korres, G.N. Optimal Allocation of Phasor Measurement Units Considering Various Contingencies and Measurement Redundancy. *IEEE Trans. Ind. Inform.* **2020**, *69*, 3403–3411. [CrossRef]
12. Chen, T.; Cao, Y.; Chen, X.; Sun, L.; Zhang, J.; Amaratunga, G.A.J. Optimal D-PMU placement approach for power systems considering non-Gaussian measurement noise statistics. *Int. J. Electr. Power Energy Syst.* **2021**, *126*, 106577. [CrossRef]
13. Khajeh, K.G.; Bashar, E.; Rad, A.M.; Gharehpetian, G. Integrated Model Considering Effects of Zero Injection Buses and Conventional Measurements on Optimal D-PMU Placement. *IEEE Trans. Smart Grid* **2017**, *8*, 1006–1013.
14. Manousakis, N.M.; Korres, G.N. Optimal PMU Placement for Numerical Observability Considering Fixed Channel Capacity—A Semidefinite Programming Approach. *IEEE Trans. Power Syst.* **2016**, *31*, 3328–3329. [CrossRef]
15. Wu, Z.; Du, X.; Gu, W.; Liu, Y.; Ling, P. Optimal D-PMU Placement Considering load loss and Relaying in Distribution Networks. *IEEE Access* **2018**, *6*, 33645–33653. [CrossRef]
16. Pei, C.; Xiao, Y.; Liang, W.; Han, X. D-PMU Placement Protection Against Coordinated False Data Injection Attacks in Smart Grid. *IEEE Trans. Ind. Appl.* **2020**, *56*, 4381–4393. [CrossRef]
17. Arpanahi, M.K.; Alhelou, H.H.; Siano, P. A Novel Multiobjective OPP for Power System Small Signal Stability Assessment Considering WAMS Uncertainties. *IEEE Trans. Ind. Inform.* **2020**, *16*, 3039–3050. [CrossRef]
18. Abdolrahim, A.; Khalil, G.F. Optimal D-PMU Placement for Power System Observability Considering Network Expansion and N-1 Contingencies. *IET Gener. Transm. Distrib.* **2018**, *18*, 4216–4224.
19. Zhu, S.; Wu, L.; Mousavian, S.; Roh, J.H. An optimal joint placement of D-PMUs and flow measurements for ensuring power system observability under N-2 transmission contingencies. *Int. J. Electr. Power Energy Syst.* **2018**, *95*, 254–265. [CrossRef]
20. Chen, X.; Wei, F.; Cao, S.; Soh, C.B.; Tseng, K.J. PMU Placement for Measurement Redundancy Distribution Considering Zero Injection Bus and Contingencies. *IEEE Syst. J.* **2020**, *14*, 5396–5406. [CrossRef]
21. Wang, S.; Liu, G.; Huang, R.; Qin, S. State Estimation Method for Active Distribution Networks Under Environment of Hybrid Measurements with Multiple Sampling Periods. *Autom. Electron. Power Syst.* **2016**, *40*, 30–36.
22. Rao, R.S.; Ravindra, K.; Satish, K.; Narasimham, S.V.L. Power Loss Minimization in Distribution System Using Network Reconfiguration in the Presence of Distributed Generation. *IEEE Trans. Power Syst.* **2013**, *28*, 317–325. [CrossRef]
23. Wu, Y.K.; Lee, C.Y.; Liu, L.C.; Tsai, S.H. Study of Reconfiguration for the Distribution System with Distributed Generators. *IEEE Trans. Power Deliv.* **2010**, *25*, 1678–1685. [CrossRef]
24. Nara, K.; Mishima, Y.; Satoh, T. Network reconfiguration for loss minimization and load balancing. In Proceedings of the 2003 IEEE Power Engineering Society General Meeting (IEEE Cat. No. 03CH37491), Toronto, ON, Canada, 13–17 July 2003; pp. 2413–2418.
25. Baran, M.E.; Wu, F.F. Network reconfiguration in distribution systems for loss reduction and load balancing. *IEEE Trans. Power Deliv.* **1989**, *4*, 1401–1407. [CrossRef]
26. Wang, Y.; Chen, Q.; Zhang, N.; Wang, Y. Conditional Residual Modeling for Probabilistic Load Forecasting. *IEEE Trans. Power Syst.* **2018**, *33*, 7327–7330. [CrossRef]
27. Deb, K.; Jain, H. An Evolutionary Many-Objective Optimization Algorithm Using Reference-Point-Based Nondominated Sorting Approach, Part I: Solving Problems With Box Constraints. *IEEE Trans. Evol. Comput.* **2014**, *18*, 577–601. [CrossRef]
28. Jain, H.; Deb, K. An Evolutionary Many-Objective Optimization Algorithm Using Reference-Point Based Nondominated Sorting Approach, Part II: Handling Constraints and Extending to an Adaptive Approach. *IEEE Trans. Evol. Comput.* **2014**, *18*, 602–622. [CrossRef]

29. Yuan, Y.; Xu, H.; Wang, B.; Yao, X. A New Dominance Relation-Based Evolutionary Algorithm for Many-Objective Optimization. *IEEE Trans. Evol. Comput.* **2016**, *20*, 16–37. [CrossRef]
30. Wang, T.C.; Lee, H.D. Developing a fuzzy TOPSIS approach based on subjective weights and objective weights. *Expert Syst. Appl.* **2009**, *36*, 8980–8985. [CrossRef]
31. Chen, Y.; Kong, X.; Yong, C.; Ma, X.; Yu, L. Distributed State Estimation for Distribution Network with Phasor Measurement Units Information. *Energy Procedia* **2019**, *158*, 4129–4134. [CrossRef]
32. Abdelsalam, H.A.; Abdelaziz, A.Y.; Osama, R.A.; Salem, R.H. Impact of Distribution System Reconfiguration on Optimal Placement of Phasor Measurement Units. In Proceedings of the 2014 Clemson University Power Systems Conference (PSC), Clemson, SC, USA, 11–14 March 2014; pp. 1–6.
33. Zhou, X.; Sun, H.; Zhang, C.; Dai, Q. Optimal placement of D-PMUs using adaptive genetic algorithm considering measurement redundancy. International Journal of Reliability. *Qual. Saf. Eng.* **2016**, *23*, 921–929.